Inorganic Chemistry

Article

pubs.acs.org/IC

Isolation and Characterization of a Dihydroxo-Bridged Iron(III,III)(μ-OH)$_2$ Diamond Core Derived from Dioxygen

Michael K. Coggins, Santiago Toledo, and Julie A. Kovacs*

The Department of Chemistry, University of Washington: Box 351700 Seattle, Washington 98195-1700, United States

Supporting Information

ABSTRACT: Dioxygen addition to coordinatively unsaturated [Fe(II)($O^{Me2}N_4$(6-Me-DPEN))](PF$_6$) (**1**) is shown to afford a complex containing a dihydroxo-bridged Fe(III)$_2$(μ-OH)$_2$ diamond core, [Fe^{III}($O^{Me2}N_4$(6-Me-DPEN))]$_2$(μ-OH)$_2$(PF$_6$)$_2$·(CH$_3$CH$_2$CN)$_2$ (**2**). The diamond core of **2** resembles the oxidized methane monooxygenase (MMOox) resting state, as well as the active site product formed following H-atom abstraction from Tyr-OH by ribonucleotide reductase (RNR). The Fe-OH bond lengths of **2** are comparable with those of the MMOHox suggesting that MMOHox contains a Fe(III)$_2$(μ-OH)$_2$ as opposed to Fe(III)$_2$(μ-OH)(μ-OH$_2$) diamond core as had been suggested. Isotopic labeling experiments with $^{18}O_2$ and CD$_3$CN indicate that the oxygen and proton of the μ-OH bridges of **2** are derived from dioxygen and acetonitrile. Deuterium incorporation (from CD$_3$CN) suggests that an unobserved intermediate capable of abstracting a H-atom from CH$_3$CN forms en route to **2**. Given the high C−H bond dissociation energy (BDE = 97 kcal/mol) of acetonitrile, this indicates that this intermediate is a potent oxidant, possibly a high-valent iron oxo. Consistent with this, iodosylbenzene (PhIO) also reacts with **1** in CD$_3$CN to afford the deuterated Fe(III)$_2$(μ-OD)$_2$ derivative of **2**. Intermediates are not spectroscopically observed in either reaction (O_2 and PhIO) even at low-temperatures (−80 °C), indicating that this intermediate has a very short lifetime, likely due to its highly reactive nature. Hydroxo-bridged **2** was found to stoichiometrically abstract hydrogen atoms from 9,10-dihydroanthracene (C−H BDE = 76 kcal/mol) at ambient temperatures.

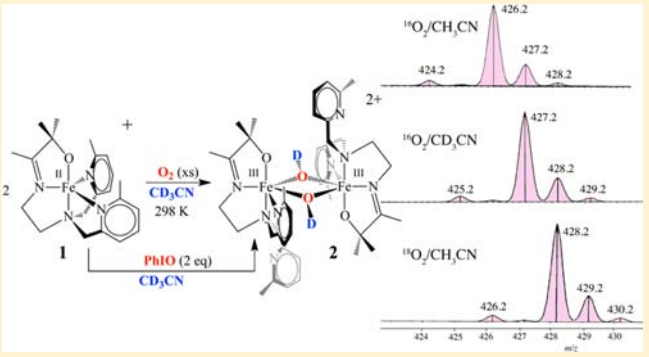

INTRODUCTION

The activation of O_2 is involved in many fundamental biochemical processes promoted by iron metalloenzymes. These transformations typically involve reactive iron-superoxo, -peroxo or high-valent oxo intermediates,[1−12] which are, in some cases, capable of activating strong C−H bonds.[1,13−15] For example, cytochrome P450 binds and subsequently activates O_2 en route to an Fe(IV)-OH porphyrin intermediate (Compound II).[13,15] Nonheme iron enzymes, such as α-ketoglutarate taurine dioxygenase (TauD)[11,16] and halogenase SyrB2,[17] activate O_2 to form high-valent Fe(IV)-oxo intermediates. The reduced binuclear Fe(II)$_2$ active site of methane monooxygenase (MMO)[1,10,18−21] and ribonucleotide reductase (RNR)[10,22−25] react with O_2 to afford highly reactive oxidized binuclear Fe(IV)$_2$(μ-O)$_2$ (A) or M(III)(μ-O)(μ-OH)M′(IV) (M, M′ = Mn, Fe; B) diamond cores,[26−28] respectively (Scheme 1), which abstract H-atoms from either CH_4 or TyrOH, respectively, to afford Fe(III)(μ-OH)(μ-O)Fe(IV) (B) or M(III)(μ-OH)$_2$M′(III) (C) species.[3,19,21,25,29,30] The highly reactive nature of these enzymatic intermediates has prompted numerous investigations aimed at establishing benchmark structural, spectroscopic, and reactivity properties of these species.[1,4,10−12,16,18−28,31−36] With RNR, the introduction of an electron along with O_2 affords structure B (Scheme 1), which in *Chlamydia tranchomatis* has been shown to contain an oxo/hydroxo bridged Fe(III)Mn(IV) dimer based on Mn and Fe K-edge EXAFS and DFT calculations.[25] It is likely that the di-iron RNRs have an analogous Fe(III)Fe(IV) core B that converts to core C upon reaction with Tyr-OH substrate (eq 1). The significantly stronger C−H bond of CH_4 requires the higher

Scheme 1

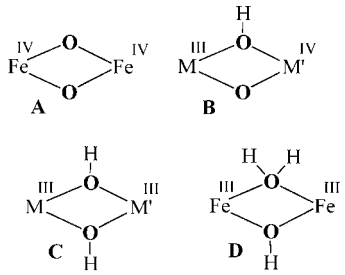

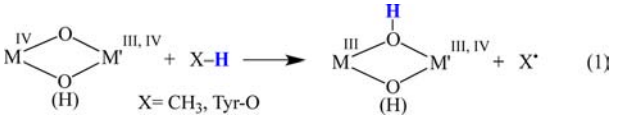

Received: May 2, 2013
Published: November 14, 2013

   dx.doi.org/10.1021/ic4010906 | Inorg. Chem. 2013, 52, 13325−13331

valent core A (Scheme 1) of methane monooxygenase (MMO) to abstract an H-atom. It has been debated as to whether the structure of the MMO oxidized resting state ($MMOH_{ox}$) contains a bis-hydroxo bridged Fe(III)(μ-OH)$_2$Fe(III) (C) or a hydroxo/aquo bridged Fe(III)(μ-OH)(μ-OH$_2$)Fe(III) (D) core.[21,37−39] One would expect the metal ion Lewis acidity of Fe(III) and Fe(IV) to disfavor protonation of a hydroxide especially if it is bridging. Water has been observed to bridge between two less Lewis acidic Fe(II) ions, however.[40]

Many of the insights regarding the reactivity structures and properties of these oxidized bimetallic diamond cores have been provided by synthetic analogues.[4,12,31−36] With synthetic complexes, solubility in nonaqueous solvents with low freezing points and small molecule crystallography can help provide mechanistic details, such as the probable identity and spectroscopic properties of reaction intermediates[18,41−45] or the location of and transfer of key protons.[46] Research efforts in our group have recently focused on the O_2 reactivity of biologically relevant first-row transition metal complexes.[47,48] Herein we describe the reactivity of a new coordinatively unsaturated Fe(II) complex with O_2 to afford a dihydroxo-bridged binuclear Fe(III) complex. Spectroscopic evidence is reported which suggests that an unobserved intermediate formed during this reaction abstracts a hydrogen atom from CH_3CN solvent.

EXPERIMENTAL SECTION

General Methods. All manipulations were performed using Schlenk line techniques or under a N_2 atmosphere in a glovebox. The highest purity reagents and solvents available were purchased and used without further purification unless otherwise noted. CH_3OH and CH_3CN (CaH_2) were dried and distilled prior to use. Et_2O was purified using solvent purification columns housed in a custom stainless steel cabinet and dispensed by a stainless steel Schlenk-line (GlassContour). CD_3CN and CD_2Cl_2 were purchased from Cambridge Isotope Laboratories, Inc. CD_3CN was either dried over CaH_2, vacuum transferred and stored in a drybox, or obtained from sealed ampules (Cambridge Isotopes (99.8%)) containing volumes small enough for a single experiment. All solvents were rigorously degassed prior to use. ^{1}H NMR spectra were recorded on either a Bruker AV 301 or Bruker AV 300 FT NMR spectrometer at ambient temperature and were referenced to residual deuterated solvent. Infrared spectra were recorded on NaCl salt plates as Nujol mulls with a Perkin-Elmer 1720 FT-IR spectrometer. Electrospray-ionization mass spectra were obtained on a Bruker Esquire Liquid Chromatograph−Ion Trap mass spectrometer. Gas chromatography−mass spectrometry data were recorded using an HP 5971A gas chromatograph interfaced with a quadrupole mass spectrometer equipped with a 7673A autosampler. Electronic absorption spectra were recorded on a Varian Cary 50 spectrophotometer equipped with a fiber optic cable connected to a "dip" ATR probe (C-technologies). A custom-built two-neck solution sample holder equipped with a threaded glass connector was sized specifically to fit the "dip" probe. Cyclic voltammograms were recorded in CH_3CN (100 mM (^{n}Bu$_4$N)(PF$_6$) supporting electrolyte) on a PAR 263A potentiostat with a glassy carbon working electrode, Ag/$AgNO_3$ reference electrode, and a platinum auxiliary electrode. EPR spectra were recorded on a Varian CW-EPR spectrometer at 15 K equipped with an Oxford helium cryostat. Solution magnetic moments were calculated by the Evans method,[49] with temperature corrections made in the manner described by Van Geet.[50] Pascal's constants were used to correct for diamagnetic contributions to the experimental magnetic moment. X-ray crystallography data was recorded on a Bruker APEX II single crystal X-ray diffractometer with Mo-radiation. Elemental analyses were performed by Atlantic Microlabs, Norcross, GA. Experiments involving iodosylbenzene were conducted using a 2 mM stock solution in CH_3OH. *N*,*N*-bis(6-methyl-2-pyridilmethyl)ethane-1,2-diamine (6-Me-DPEN) was prepared according to literature procedures.[48]

Synthesis of [Fe^{II}(O^{Me2}N$_4$(6-Me-DPEN))](PF$_6$) (1). $FeCl_2$ (0.094 g, 0.74 mmol), *N*,*N*-bis(6-methyl-2-pyridilmethyl)ethane-1,2-diamine (0.20 g, 0.74 mmol), 3-hydroxy-3-methyl-2-butanone (0.09 g, 0.86 mmol), $NaOCH_3$ (0.40 g, 0.74 mmol), and $NaPF_6$ (0.12 g, 0.74 mmol) were combined in CH_3OH (10 mL) and allowed to stir under an inert atmosphere in a glovebox at room temperature for two days. All volatiles were then removed *in vacuo* to yield a crude yellow solid, which was recrystallized from CH_3CN/Et_2O at 258 K to yield the title compound as a bright yellow solid in 47% yield (0.20 g, 0.35 mmol). Electronic absorption spectrum: λ_{max} (nm) (ε (M^{-1} cm^{-1})) (CH_3CN): 412 (250). Redox potential (CH_3CN vs $Fc^{+/0}$, 298 K): E_{pa} = +230 mV, E_{pc} = +10 mV, ΔE = 220 mV. Magnetic moment (299 K, CD_3OD solution): 4.71 μ_B. ESI-MS: Expected m/z for $[C_{21}H_{29}N_4OFe]^+$ = 409.3, found m/z = 409.2. Elemental analysis results were obtained with the BPh_4^- salt of **1**, which was synthesized by the same procedure described above except that $NaBPh_4$ was used instead of $NaPF_6$. Elemental analysis for $C_{45}H_{49}N_4BOFe$; Calculated C, 72.06; H, 7.16; N, 6.86. Found C, 71.11; H, 7.60; N, 6.41.

Synthesis of [Fe^{III}(O^{Me2}N$_4$(6-Me-DPEN))]$_2$(μ-OH)$_2$(PF$_6$)$_2$·(CH$_3$CH$_2$CN)$_2$ (2). Complex **1** (0.20 g, 0.36 mmol) was dissolved in CH_3CN (5 mL) under an inert atmosphere in a glovebox at room temperature. The resulting solution was placed into a gastight syringe, removed from the glovebox, and injected into a custom-made two-neck vial equipped with a septum cap that had previously been purged with argon and contained a stir bar. Dioxygen, from a pressurized tank (Praxair, 99.9999%, <0.5 ppm H_2O) and run through a column of anhydrous $CaSO_4$ (Drierite), was gently bubbled into the stirring solution for approximately five minutes. The reaction mixture was allowed to continue stirring at room temperature for two hours, during which time the solution had turned from yellow to dark orange. All volatiles were then removed *in vacuo* to yield a dark orange solid, which was recrystallized from CH_3CN/Et_2O (1/6 vol/vol) at 253 K to afford the title compound in 96% yield (0.19 g, 0.17 mmol). X-ray quality crystals of **2** were grown from a concentrated CH_3CH_2CN solution at −80 °C, as well as from a concentrated CH_3CN solution at room temperature. FT-IR (NaCl plates, Nujol mull, 298 K): ν(O−H) = 3610 cm^{-1}; ν(O−D) = 2730 cm^{-1}. Elemental analysis for $C_{42}H_{58}N_8O_4F_{12}P_2Fe_2$; Calculated C, 44.50; H, 5.69; N, 10.61. Found C, 45.84; H, 5.33; N, 10.40.

Characterization of 2 in CH$_3$CN Solution. Electronic absorption spectrum: λ_{max} (nm) (ε (M^{-1} cm^{-1})): 310 (610), 375 (br, 440) (extinction coefficients calculated per Fe(III)). Redox potential (CH_3CN vs $Fc^{+/0}$, 298 K): E_{pa} = +235 mV, E_{pc} = +26 mV. Magnetic moment (300 K, CD_3CN solution): 5.82 μ_B/Fe(III). ESI-MS: Expected m/z for $[C_{21}H_{30}N_4O_2Fe]^+$ = 426.3, found m/z = 426.2. Expected m/z for $[C_{21}H_{29}DN_4O_2Fe]^+$ = 427.3, found m/z = 427.2. Expected m/z for $[C_{21}H_{30}N_4O^{18}OFe]^+$ = 428.3, found m/z = 428.2. EPR spectrum (1:1 CH_3CN/toluene glass, 14 K): g = 1.96, 4.07, 10.2.

Synthesis and Isolation of Deuterium Labeled [Fe^{III}(O^{Me2}N$_4$(6-Me-DPEN))]$_2$(μ-OD)$_2$(PF$_6$)$_2$·(CH$_3$CH$_2$CN)$_2$ (2) for FT-IR Experiments. *Method 1.* A solution of **1** (0.25 g, 0.45 mmol) was prepared in dry CD_3CN (30 mL; Cambridge Isotopes (99.8%)) under an inert atmosphere in a glovebox. The resulting solution was placed into a gastight syringe, removed from the glovebox, and injected into a custom-made two-neck vial equipped with a septum cap that had previously been purged with argon and contained a stir bar. Dioxygen, derived from a pressurized tank (Praxair, 99.9999%, <0.5 ppm H_2O) and run through a column of anhydrous $CaSO_4$ (Drierite), was gently bubbled into the stirring solution for approximately five minutes. The reaction was allowed to continue to stir at room temperature for 30 min, after which all volatiles were removed *in vacuo* to afford **2** as a dark orange solid. The resulting solid was redissolved in a minimal amount of CH_3CH_2CN and crystallized at −80 °C. Crystalline samples of **2** were harvested from the mixture via filtration through a fine fritted filter, briefly dried *in vacuo* at room temperature, and subsequently used for FT-IR experiments.

Method 2. A solution of **2** (0.090 g, 0.16 mmol) was prepared in dry CH_3CN (10 mL) under aerobic conditions at room temperature. D_2O (0.1 mL) was added to this solution, and the resulting reaction mixture was allowed to gently stir at room temperature overnight. All volatiles were then removed *in vacuo* to afford a dark orange solid, which was left under vacuum for 72 h. The solid was then redissolved

dx.doi.org/10.1021/ic4010906 | Inorg. Chem. 2013, 52, 13325−13331

in a minimal amount of CH_3CH_2CN, crystallized at −80 °C, harvested via filtration, and subsequently used for FT-IR experiments.

Analysis of Products From Reactions Between Complex 2 and 9,10-Dihydroanthracene in CH_3CN. In a typical reaction, **2** was dissolved in CH_3CN (3−4 mL, ∼0.5 mM solution of **2**) at room temperature under an inert atmosphere in a glovebox. The resulting solution was placed into a gastight syringe, removed from the glovebox, and injected into a custom-made two-neck vial containing a stir bar and equipped with a septum cap and threaded dip-probe feed-through adaptor that had previously been purged with Ar. 9,10-Dihydroanthracene (0.5 equivalents per Fe(III)) was then added to the solution in a similar fashion from a concentrated stock solution that had been prepared in CH_3CN in a glovebox. Each reaction mixture (the reaction was repeated three times and shown to be reproducible in all three cases) was allowed to stir under anaerobic conditions for 10−15 min, and then dried *in vacuo*. The solid products were then washed with Et_2O (3 mL) and the Et_2O soluble components were subsequently analyzed by GC/MS and quantified using standard calibration curves.

X-ray Crystallography. A yellow crystal of **1** with dimensions 0.05 × 0.04 × 0.4 mm^3 was mounted on a glass capillary with oil. Data was collected at −143 °C. The crystal-to-detector distance was set to 30 mm and exposure time was 60 s per degree for all sets of exposure. The scan width was 2.0°. Data collection was 99.4% complete to 25.0° in ϑ. A total of 56,116 partial and complete reflections were collected covering the indices, h = −21 to 21, k = −19 to 19, l = −32 to 32. 69,506 reflections were symmetry independent and the R_{int} = 0.125 indicated that the data was poor. Indexing and unit cell refinement indicated an orthorhombic P lattice with the space group *Pbca* (No. 61).

A pale red plate of **2** with dimensions 0.20 × 0.10 × 0.10 mm^3 was mounted on a glass capillary with oil. Data was collected at −173 °C. The crystal-to-detector distance was set to 40 mm and exposure time was 30 s per degree for all sets of exposure. The scan width was 0.5°. Data collection was 99.9% complete to 25.0° in ϑ. A total of 51,770 partial and complete reflections were collected covering the indices, h = −15 to 14, k = −15 to 15, l = −17 to 17. 7,264 reflections were symmetry independent and the R_{int} = 0.0512 indicated that the data was good. Indexing and unit cell refinement indicated a triclinic P lattice with the space group P−1 (No. 2).

All data was integrated and scaled using SAINT, SADABS within the APEX2 software package by Bruker. Solutions by direct methods (SHELXS, SIR97) produced complete heavy atom phasing models which were consistent with each proposed structure. Scattering factors are from Waasmair and Kirfel.[51] Crystal data for **1** and **2** are provided in Table 1. All non-hydrogen atoms were refined anistropically by full-matrix least-squares methods. Most hydrogen atoms were placed using a riding model; however, the hydrogen atoms on the bridging hydroxide ligands in **2** were refined from the difference map. Crystallographic data is summarized in Table 1. Selected distances and angles are summarized in Table 2.

RESULTS AND DISCUSSION

Synthesis and Structure of Coordinatively Unsaturated Fe(II) Alkoxide Complex. The alkoxide-ligated complex $[Fe^{II}(O^{Me2}N_4(6\text{-Me-DPEN}))](PF_6)$ (**1**) was synthesized via an Fe(II)-templated Schiff-base condensation between 6-Me-DPEN[48] and 3-hydroxy-3-methyl-2-butanone in CH_3OH under an inert atmosphere at ambient temperature. X-ray quality crystals of **1** were obtained via vapor diffusion of Et_2O into a saturated CH_3CN solution at room temperature. As shown in the ORTEP diagram of Figure 1, the Fe(II) ion of **1** is found in a distorted trigonal bipyramidal coordination environment (τ = 0.61)[52] comprising an alkoxide oxygen (O(1)), imine nitrogen (N(1)), tertiary amine (N(2)), and two pyridine nitrogens (N(3) and N(4)) (Figure 1). Coordinatively unsaturated **1** is high-spin (S = 2, μ_{eff} = 4.71 μ_B in CD_3OD) and exhibits a quasi-reverisble $Fe^{III/II}$ redox couple in CH_3CN (under nitrogen) with $E_{1/2}$ = +120 mV vs $Fc^{+/0}$ (ΔE = 220 mV, Figure S-1).

Table 1. Crystal Data for $[Fe^{II}(O^{Me2}N_4(6\text{-Me-DPEN}))](PF_6)$ (1) and $[Fe^{III}(O^{Me2}N_4(6\text{-Me-DPEN}))]_2(\mu\text{-OH})_2(PF_6)_2\cdot(CH_3CH_2CN)_2$ (2)

	1	2
Formula	$C_{21}H_{29}F_6FeN_4OP$	$C_{48}H_{70}F_{12}Fe_2N_{10}O_4P_2$
MW	553.40	1252.78
T, K	130(2)	100(2)
Unit Cell	Orthorhombic	Triclinic
a, Å	15.9090(11)	11.237(2)
b, Å	17.1316(12)	11.403(2)
c, Å	17.6610(13)	13.334(2)
α, deg	90	70.554(9)
β, deg	90	66.281(9)
γ, deg	90	87.391(10)
V, Å^3	4813.3(6)	1467.3(5)
Z	8	1
d (calc), g/cm^3	1.530	1.418
Space group	*Pbca*	P−1
R	0.0592	0.0366
R_w	0.1548	0.0796
GOF	0.928	1.007

Table 2. Selected Bond Distances (Å) and Bond Angles (deg) for $[Fe^{II}(O^{Me2}N_4(6\text{-Me-DPEN}))](PF_6)$ (1) and $[Fe^{III}(O^{Me2}N_4(6\text{-Me-DPEN}))]_2(\mu\text{-OH})_2(PF_6)_2\cdot(CH_3CH_2CN)_2$ (2)

	1	2
Fe(1)−O(1)	1.925(3)	1.8721(13)
Fe(1)−N(1)	2.086(4)	2.1121(15)
Fe(1)−N(2)	2.273(5)	2.2556(15)
Fe(1)−N(3)	2.139(4)	2.2144(16)
Fe(1)−N(4)	2.121(4)	N/A
Fe(1)−O(2)	N/A	1.9715(13)
Fe(1′)−O(2)	N/A	2.0037(14)
Fe(1)···Fe(1′)[a]	N/A	3.172
O(1)−Fe−N(1)	78.97(16)	78.34(6)
O(1)−Fe−N(2)	154.82(15)	148.61(5)
O(1)−Fe−N(3)	117.97(16)	98.17(6)
O(1)−Fe−N(4)	116.24(16)	N/A
N(1)−Fe−N(3)	116.03(17)	107.26(6)
N(1)−Fe−N(4)	122.64(17)	N/A
N(3)−Fe−N(4)	104.41(15)	N/A
O(1)−Fe−O(2)	N/A	106.24(5)
O(1)−Fe−O(2′)	N/A	104.88(6)
N(1)−Fe−O(2)	N/A	163.94(6)
Fe(1)−O(2)−Fe(1′)	N/A	105.88(6)
O(2)−Fe(1)−O(2#)	N/A	74.12(6)

[a]Fe(1) and Fe(1′) and O(2) and O(2′) are equivalent in **2** and related by a crystallographically imposed inversion center, i.e., only one-half of the dimer is crystallographically independent.

The room temperature electronic absorption spectrum of **1** in CH_3CN contains a single absorption band with λ_{max} =412 nm (ε = 250 M^{-1} cm^{-1} Figure S-2).

Reactivity with Dioxygen to Afford Dihydroxo-Bridged Iron(III,III)(μ−OH)$_2$ Diamond Core. If excess amounts of dry O_2, derived from a pressurized tank (Praxair, 99.9999%, <0.5 ppm H_2O) and dried via a column of anhydrous $CaSO_4$ (Drierite), are bubbled into a CH_3CN solution of **1** for ∼2−3 min at ambient temperature the solution changes from yellow to dark orange, a broad band at λ_{max} = 310 nm (Figure S-3) grows in in the electronic absorption spectrum, and the broad band at 412 nm (Figure S-2) disappears.

dx.doi.org/10.1021/ic4010906 | Inorg. Chem. 2013, 52, 13325−13331

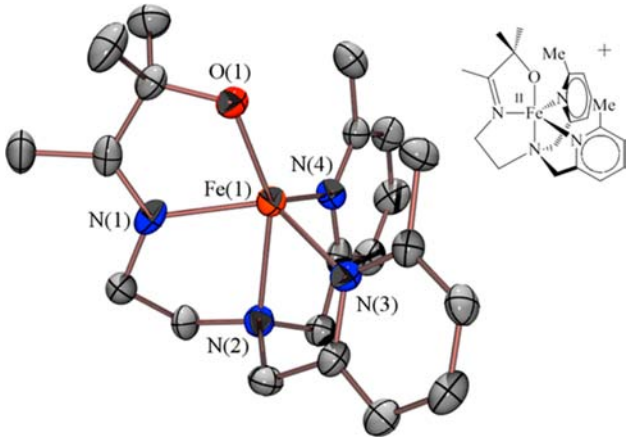

Figure 1. ORTEP diagram (50% probability) of $[Fe^{II}(O^{Me2}N_4(6\text{-Me-DPEN}))]^+$ (**1**) with hydrogen atoms and counterion omitted for clarity.

Low temperature reactions were also performed at either −40 °C in CH_3CN or −80 °C in CH_3CH_2CN; however, no transient intermediates were observed under these conditions. X-ray quality crystals of the orange product obtained from this reaction, $[Fe^{III}(O^{Me2}N_4(6\text{-Me-DPEN}))]_2(\mu\text{-OH})_2(PF_6)_2\cdot(CH_3CH_2CN)_2$ (**2**), were obtained in high yield (96%) via vapor diffusion of Et_2O into a concentrated CH_3CH_2CN solution at −80 °C (Figure S-4). As shown in the ORTEP diagram of Figure 2, both Fe(III) ions of

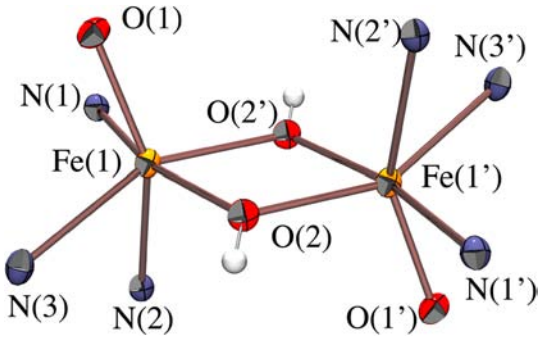

Figure 2. ORTEP diagram (50% probability) of the Fe(III)(μ-OH)$_2$Fe′(III) diamond core and Fe coordination sphere of dicationic-$\{[Fe^{III}(O^{Me2}N_4(6\text{-Me-DPEN}))]_2(\mu\text{-OH})_2\}^{2+}$ (**2**). The two halves of the molecule are related by a crystallographic inversion center. An ORTEP diagram of the entire dicationic complex is shown in Figure S-4.

2 are located in a distorted octahedral environment consisting of an alkoxide oxygen (O(1)), two hydroxide bridging ligands (O(2) and O(2′)), an imine nitrogen (N(1)), a tertiary amine (N(2)), and a pyridine nitrogen (N(3)) (Figure 2). The location and refinement of a hydrogen atom on each of the bridging oxygen atoms (O(2)) in the X-ray structure, along with the presence of two PF_6^- counterions per diiron complex, conclusively identified the bridging ligands of **2** as hydroxides. Hydrogen-bonding interactions ((O(2)-H···N(21)) = 2.200 Å; O(2)−H−N(21)= 171.29°) between the bridging hydroxide ligands and co-crystallized CH_3CH_2CN nitrogens (Figure S-4) further verified this assignment.

The hydroxide ligands in **2** are asymmetrically bridging with Fe(1)−O(2) and Fe(1)-O(2′) bond lengths of 1.9715(13) Å and 2.0037(14) Å, respectively (Table 2). These distances are comparable to other structurally characterized Fe(III)$_2$(μ-OH)$_2$ and Fe(III)$_2$(μ-OH)$_2$(μ-O_2CR) complexes (1.88−2.08 Å).[35,36,53−64] The Fe(1)···Fe(1′) distance in **2** (3.172 Å) is, on the other hand, longer than the reported Fe(III)$_2$(μ-OH)$_2$ core range (3.07−3.12 Å), while the Fe(1)−O(2)−Fe(1′) bridging angle 105.88(6)° is at the larger end of the previously reported range (92.3−105.8°).[53−63] This likely results from steric congestion around each of the two Fe(III) ions, as is further indicated by the dissociation of a pyridine arm away from each metal ion in both halves of the dimer (Figure S-4).

Isotopic Labeling Experiments. Isotopic labeling studies conducted with $^{18}O_2$ confirmed that the two bridging hydroxide ligands in **2** are indeed derived from O_2 (Scheme 2; Figure S-5−

Scheme 2

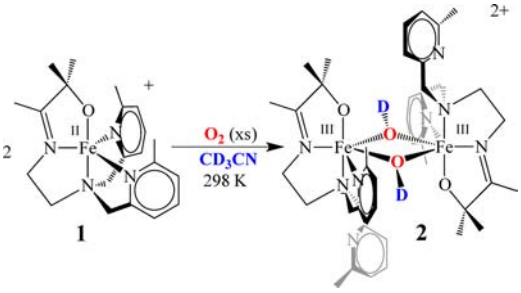

Figure S-7). As shown by the Fe-isotope distribution pattern in the ESI mass spectra of Figure 3a, the μ-hydroxo bridge cleaves in the mass spectrometer to afford a monomeric monocationic Fe-hydroxo species with a parent ion m/z peak at 426.2 (Figure S-5), which corresponds to half of the $\{[Fe^{III}(O^{Me2}N_4(6\text{-Me-DPEN}))]_2(\mu\text{-OH})_2\}^{2+}$ dimer **2**, $[Fe^{III}(O^{Me2}N_4(6\text{-Me-DPEN}))(OH)]^+$, and is 17 mass units greater than that (m/z = 409.2) of **1** (Figure S-6). This parent ion peak (at m/z = 426.2; Figure 3a) shifts by two mass units (to m/z = 428.2; Figure 3c) upon the incorporation of ^{18}O from ^{18}O-labeled dioxygen (Figure S-7). In order to determine the source of the hydrogen atoms found on the hydroxide bridging ligands in **2**, deuterium labeling studies were conducted. If O_2 is added to **1** in deuterated acetonitrile (CD_3CN), then a parent ion peak at m/z = 427.2 (Figure 3b), which is shifted by one mass unit (Figure S-8) relative to that observed at m/z = 426.2 (Figure 3a) in the CH_3CN reaction (Figure S-5), is observed consistent with the incorporation of deuterium. Again, the Fe-isotope distribution pattern indicates that the bis-hydroxo bridged di-iron complex cleaves in the mass spectrometer to afford a monomeric $[Fe^{III}(O^{Me2}N_4(6\text{-Me-DPEN}))(OD)]^+$. Although one cannot rule out some sort of impurity in the CD_3CN as the source of deuterium, it is unlikely that D_2O from "wet" CD_3CN is responsible, given that the ^{18}O-label in the spectrum of Figure 3c is not "washed out" via exchange with water ($H_2{}^{16}O$) contamination in the CH_3CN. It is also unlikely that D_2O, as opposed to H_2O, would be a contaminant in the CD_3CN. Deuterium labeled **2** was also obtained from a reaction between **1** and O_2 in CD_2Cl_2. Additional evidence to support the incorporation of deuterium from CD_3CN is shown by the vibrational spectrum (Figure S-9) of crystalline **2** (synthesized in CH_3CN), which displays a sharp feature at 3610 cm^{-1} that shifts to 2730 cm^{-1} when **2** is synthesized in CD_3CN. The energies and observed isotopic shift (ν_{O-H}/ν_{O-D} = 1.32 vs theoretical = 1.35) for these vibrational features are consistent with O−H and O−D stretches, respectively.

Implications Regarding the Involvement of a Reactive Intermediate. Deuterium incorporation (from CD_3CN) suggests that an unobserved intermediate capable of abstracting

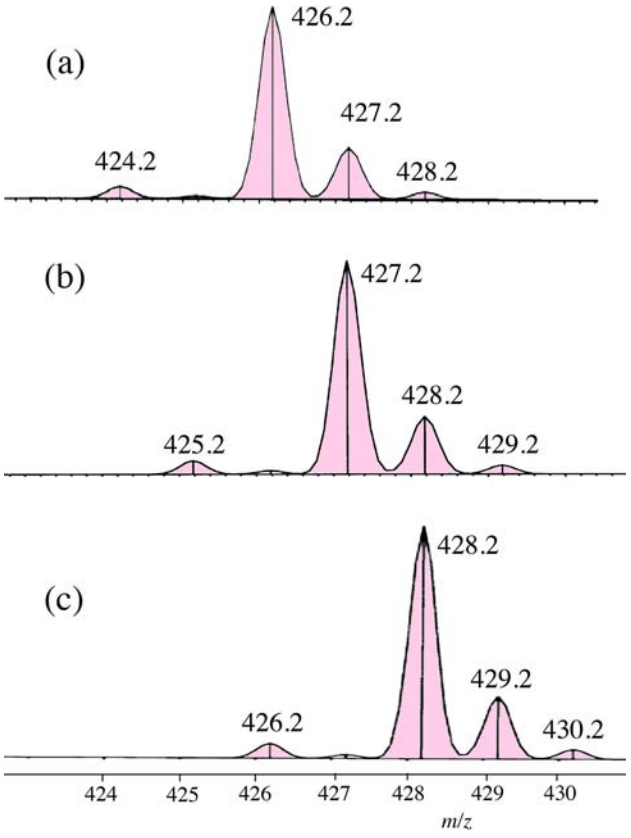

Figure 3. ESI-MS of the cleaved monomeric product observed when dicationic $\{[Fe^{III}(O^{Me2}N_4(6\text{-Me-DPEN}))]_2(\mu\text{-OH})_2^{2+}$ (**2**), obtained from (a) the reaction between **1** and $^{16}O_2$ in CH_3CN, (b) the reaction between **1** and $^{16}O_2$ in CD_3CN, and (c) the reaction between **1** and $^{18}O_2$ in CH_3CN, is placed in the mass spectrometer.

an H-atom from CH_3CN forms in the dioxygen reaction (Scheme 2) en route to **2**. Given the high C−H bond dissociation energy (BDE = 97 kcal/mol) of acetonitrile, this indicates that this intermediate is a potent oxidant, possibly a high-valent iron oxo. Consistent with this, iodosylbenzene (PhIO) also reacts with **1** in CD_3CN (Scheme 3) to afford the deuterated $Fe(III)_2(\mu\text{-OD})_2$ derivative of **2** (93−96% yield), as verified by FT-IR (ν_{O-D}= 2727 cm^{-1}; Figure S-11) and ESI-MS (m/z = 427.2; Figure S-10). Intermediates are not spectroscopically observed in either reaction (O_2 and PhIO) even at low temperatures (−80 °C), indicating that this intermediate has a very short lifetime, likely due to its highly reactive nature. Iodosylbenzene (PhIO) would be expected to afford a Fe(IV)═O upon its reaction with Fe(II) (Scheme 3).[65−69] High-valent Fe(IV)═O species have been shown to be highly reactive and capable of abstracting H-atoms, especially in the presence of anionic ligands.[68−73] Hydrogen atom abstraction from acetonitrile has been previously observed during the O_2-promoted oxidation of $[Mn(II)1^{cyp}]^{1-}$ to $[Mn(III)1^{cyp}(OH)]^{1-}$ via a high-valent Mn-oxo intermediate.[74] High-valent iron oxo compounds $[Fe(IV)(O)BnTPEN)]^{2+}$,[75] $[Fe(IV)(PY5)(O)]^{2+}$,[76] and aqueous $Fe(IV)O^{2+}$ have also been shown to abstract hydrogen atoms from CH_3CN.[77]

Reactivity of Dihydroxo-Bridged 2 with Substrates Containing Weaker C−H Bonds. The reactivity of the dihydroxo-bridged product **2** toward stoichiometric amounts of substrates containing relatively weak C−H bonds was explored under anaerobic conditions in CH_3CN at room temperature. Under these conditions, 9,10-dihydroanthracene (C−H BDFE = 76.0 kcal·mol^{-1})[78] was

Scheme 3

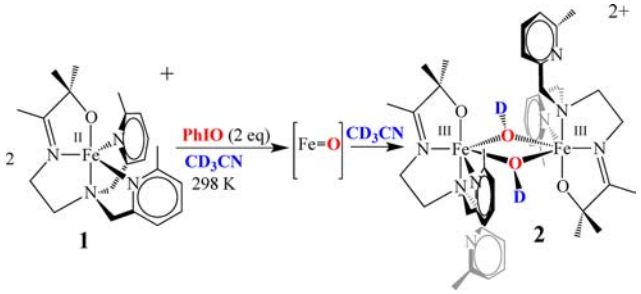

oxidized to anthracene in 23(3)% yield (Figures S-12, S-13). Complex **2** was unreactive, however, with organic compounds containing stronger C−H bonds, such as toluene and cyclohexane (C−H BDFE = 87 kcal·mol^{-1} and 99 kcal·mol^{-1}, respectively).[78] This reactivity is similar to other Fe(III)-OH species, such as lipoxygenase[79,80] and $[Fe^{III}(PY5)(OH)]^{2+}$,[76] which have been found to abstract hydrogen atoms from substrates containing relatively weak C−H bonds.

CONCLUSIONS

In conclusion, we have described the synthesis and characterization of a new coordinatively unsaturated Fe(II) complex (**1**) that reacts with O_2 to form an $Fe(III)_2(\mu\text{-OH})_2$ diamond core (**2**) in high yield. Isotopic labeling studies suggest that an unobserved intermediate formed during the conversion of **1** to **2** is capable of oxidizing CH_3CN, presumeably via $H^{\bullet}$ atom transfer. Iodosylbenzene (PhIO, 1.0 equiv) also oxidizes **1** to afford **2** in high yield in CH_3CN. Although low temperature intermediates were not observed during reactions between **1** and either O_2 or PhIO, an unobserved high-valent Fe(IV)═O intermediate, that is capable of, and responsible for, the observed solvent oxidation, is proposed in both of these reactions. Reactivity studies also showed that hydroxo-bridged **2** is itself also capable of oxidizing the relatively weak C−H bonds of DHA at room temperature. Efforts toward further exploration of this reactivity, as well as comparing the properties and reactivity of thiolate-ligated analogues, are currently underway.

ASSOCIATED CONTENT

Supporting Information

Cyclic voltammogram, electronic absorption spectrum, and ESI-MS data for **1**, and ESI-MS data for **2**, and isotopic (^{18}O and D) derivatives thereof, derived from O_2 and PhIO in CH_3CN or CD_3CN. More detailed ORTEP diagram of **2**, along with crystallographic tables of both **1** and **2**. This material is available free of charge via the Internet at http://pubs.acs.org.

AUTHOR INFORMATION

Corresponding Author

*E-mail: kovacs@chem.washington.edu. Tel. (206)543-0713. FAX (206)685-8665.

Notes

The authors declare no competing financial interest.

ACKNOWLEDGMENTS

NIH funding (#RO1GM45881-20) is gratefully acknowledged.

REFERENCES

(1) Tinberg, C. E.; Lippard, S. J. *Acc. Chem. Res.* **2011**, *44*, 280−288.
(2) Kovaleva, E. G.; Lipscomb, J. D. *Science* **2007**, *316*, 453−456.

(3) Feig, A. L.; Lippard, S. J. *Chem. Rev.* **1994**, *94*, 759−805.
(4) Costas, M.; Mehn, M. P.; Jensen, M. P.; Que, L. J. *Chem. Rev.* **2004**, *104*, 939−986.
(5) Cho, J.; Jeon, S.; Wilson, S. A.; Liu, L. V.; Kang, E. A.; Braymer, J. J.; Lim, M. H.; Hedman, B.; Hodgson, K. O.; Valentine, J. S.; Solomon, E. I.; Nam, W. *Nat. Chem.* **2011**, *478*, 502−505.
(6) Krebs, C.; Fujimori, D. G.; Walsh, C. T.; Bollinger, J. M., Jr. *Acc. Chem. Res.* **2007**, *40*, 484−492.
(7) Kovaleva, E. G.; Neibergall, M. B.; Chakrabarty, S.; Lipscomb, J. D. *Acc. Chem. Res.* **2007**, *40*, 475−483.
(8) Que, L., Jr. *Acc. Chem. Res.* **2007**, *40*, 493−500.
(9) Kovacs, J. A. *Science* **2003**, *299*, 1024−1025.
(10) Solomon, E. I.; Brunold, T. C.; Davis, M. I.; Kemsley, J. N.; Lee, S. K.; Lehnert, N.; Neese, F.; Skulan, A. J.; Yang, Y. S.; Zhou, J. *Chem. Rev.* **2000**, *100*, 233−349.
(11) Price, J. C.; Barr, E. W.; Tirupati, B.; Bollinger, J. M., Jr.; Krebs, C. *Biochemistry* **2003**, *42*, 7497−7508.
(12) Que, L.; Tolman, W. B. *Nature* **2008**, *455*, 333−340.
(13) Rittle, J.; Green, M. T. *Science* **2010**, *330*, 933−937.
(14) Borovik, A. S. *Chem. Soc. Rev.* **2011**, *40*, 1870−1874.
(15) Sono, M.; Roach, M. P.; Coulter, E. D.; Dawson, J. H. *Chem. Rev.* **1996**, *96*, 2841−2887.
(16) Elkins, J. M.; Ryle, M. J.; Clifton, I. J.; Hotopp, J. C. D.; Lloyd, J. S.; Burzlaff, N. I.; Baldwin, J. E.; Hausinger, R. P.; Roach, P. L. *Biochemistry* **2002**, *41*, 5185−5192.
(17) Matthews, M. L.; Krest, C. M.; Barr, E. W.; Vaillancourt, F. H.; Walsh, C. T.; Green, M. T.; Krebs, C.; Bollinger, J. M., Jr. *Biochemistry* **2009**, *48*, 4331−4343.
(18) Xue, G.; Fiedler, A. T.; Martinho, M.; Munck, E.; Que, L., Jr. *Proc. Natl. Acad. Sci. U.S.A.* **2008**, *105*, 20615−20620.
(19) Valentine, A. M.; Stahl, S. S.; Lippard, S. J. *J. Am. Chem. Soc.* **1999**, *121*, 3876−3887.
(20) Liu, K. E.; Valentine, A. M.; Wang, D.; Huynh, B. H.; Edmondson, D. E.; Salifoglou, A.; Lippard, S. J. *J. Am. Chem. Soc.* **1995**, *117*, 10174−10185.
(21) Merkx, M.; Kopp, D. A.; Sazinsky, M. H.; Blazyk, J. L.; Müller, J.; Lippard, S. J. *Angew. Chem., Int. Ed.* **2001**, *40*, 2782−2807.
(22) Bollinger, J. M., Jr.; Tong, W. H.; Ravi, N.; Huyuh, B. H.; Edmondson, E. D.; Stubbe, J. *J. Am. Chem. Soc.* **1994**, *116*, 8015−8023.
(23) Bollinger, J. M., Jr.; Edmondson, D. E.; Huynh, B. H.; Filley, J.; Norton, J. R.; Stubbe, J. *Science* **1991**, *253*, 292−298.
(24) Cotruvo, J. A., Jr.; Stich, T. A.; Britt, R. S.; Stubbe, J. *J. Am. Chem. Soc.* **2013**, *135*, 4027−4039.
(25) Younker, J. M.; Krest, C. M.; Jiang, W.; Krebs, C.; Bollinger, J. M., Jr; Green, M. T. *J. Am. Chem. Soc.* **2008**, *130*, 15022−15027.
(26) Xue, G.; Geng, C.; Ye, S.; Fiedler, A. T.; Neese, F.; Que, L., Jr. *Inorg. Chem.* **2013**, *52*, 3976−3984.
(27) Lee, S.-K.; Nesheim, J. C.; Lipscomb, J. D. *J. Biol. Chem.* **1993**, *268*, 21569−21577.
(28) Que, L. J.; Tolman, W. B. *Angew. Chem., Int. Ed.* **2002**, *41*, 1114−1137.
(29) Brunold, T. C. *Proc. Natl. Acad. Sci. U.S.A.* **2007**, *104*, 20641−20642.
(30) Tshuva, E. Y.; Lippard, S. J. *Chem. Rev.* **2004**, *104*, 987−1012.
(31) Decker, A.; Solomon, E. I. *Angew. Chem., Int. Ed.* **2005**, *44*, 2252−2255.
(32) Xue, G.; Wang, D.; De Hont, R.; Fiedler, A. T.; Shan, X.; Munck, E.; Que, L., Jr. *Proc. Natl. Acad. Sci. U.S.A.* **2007**, *104*, 20173−20178.
(33) Borovik, A. S. *Acc. Chem. Res.* **2005**, *38*, 54−61.
(34) Shook, R. L.; Peterson, S. M.; Greaves, J.; Moore, C.; Rheingold, A. L.; Borovik, A. S. *J. Am. Chem. Soc.* **2011**, *133*, 5810−5817.
(35) Lee, D.; Lippard, S. J. *J. Am. Chem. Soc.* **1998**, *120*, 12153−12154.
(36) Lee, D.; Lippard, S. J. *J. Am. Chem. Soc.* **2001**, *123*, 4611−4612.
(37) Tinberg, C. E.; Lippard, S. J. *Biochemistry* **2010**, *49*, 7902−7912.
(38) Elango, N.; Radhakrishnan, R.; Forland, W. A.; Wallar, B. J.; Earhart, C. A.; Lipscomb, J. D.; Ohlendorf, D. H. *Protein Sci.* **1997**, *6*, 556−568.
(39) Rosenzweig, A. C.; Nordlund, P.; Takahara, P. M.; Frederick, C. A.; Lippard, S. J. *Chem. Biol.* **1995**, *2*, 409−418.
(40) Hagen, K. S.; Lachicotte, R. *J. Am. Chem. Soc.* **1992**, *114*, 8741−8742.
(41) Kodera, M.; Kawahara, Y.; Hitomi, Y.; Nomura, T.; Ogura, T.; Kobayashi, Y. *J. Am. Chem. Soc.* **2012**, *134*, 13236−13239.
(42) Kim, K.; Lippard, S. L. *J. Am. Chem. Soc.* **1996**, *118*, 4914−4915.
(43) Dong, Y.; Menage, S.; Brennan, B. A.; Elgren, T. E.; Jang, H. G.; Pearce, L. L.; Que, L. J. *J. Am. Chem. Soc.* **1993**, *115*, 1851−1859.
(44) Shook, R. L.; Gunderson, W. A.; Greaves, J.; Ziller, J. W.; Hendrich, M. P.; Borovik, A. S. *J. Am. Chem. Soc.* **2008**, *130*, 8888−8889.
(45) MacBeth, C. E.; Golombek, A. P.; Young, V. G., Jr.; Yang, C.; Kuczera, K.; Hendrich, M. P.; Borovik, A. S. *Science* **2000**, *289*, 938−941.
(46) Shearer, J.; Scarrow, R. C.; Kovacs, J. A. *J. Am. Chem. Soc.* **2002**, *124*, 11709−11717.
(47) Theisen, R. M.; Shearer, J.; Kaminsky, W.; Kovacs, J. A. *Inorg. Chem.* **2004**, *43*, 7682−7690.
(48) Coggins, M. K.; Sun, X.; Kwak, Y.; Solomon, E. I.; Rybak-Akimova, E. V.; Kovacs, J. A. *J. Am. Chem. Soc.* **2013**, *135*, 5631−5640.
(49) Evans, D. A. *J. Chem. Soc.* **1959**, 2005.
(50) Van Geet, A. L. *Anal. Chem.* **1968**, *40*, 2227−2229.
(51) Waasmaier, D.; Kirfel, A. *Acta Crystallogr., Sect. A* **1995**, *51*, 416.
(52) Addison, A. W.; Rao, T. N.; Reedijk, J. *J. Chem. Soc., Dalton Trans.* **1984**, 1349−1356.
(53) Matsumoto, K.; Egami, H.; Oguma, T.; Katsuki, T. *Chem. Commun.* **2012**, *48*, 5823−5825.
(54) Bruijnincx, P. C. A.; Buurmans, I. L. C.; Huang, Y.; Juhász, G.; Viciano-Chumillas, M.; Quesada, M.; Reedijk, J.; Lutz, M.; Spek, A. L.; Münck, E.; Bominaar, E. L.; Gebbink, R. J. M. K. *Inorg. Chem.* **2011**, *50*, 9243−9255.
(55) Safaei, E.; Sheykhi, H.; Weyhermüller, T.; Bill, E. *Inorg. Chim. Acta* **2011**, *384*, 69−75.
(56) Egami, H.; Matsumoto, K.; Oguma, T.; Kunisu, T.; Katsuki, T. *J. Am. Chem. Soc.* **2010**, *132*, 13633−13635.
(57) Boudalis, A. K.; Clemente-Juan, J. M.; Dahan, F.; Psycharis, V.; Raptopoulou, C. P.; Donnadieu, B.; Sanakis, Y.; Tuchagues, J.-P. *Inorg. Chem.* **2008**, *47*, 11314−11323.
(58) Ghiladi, M.; Larsen, F. B.; McKenzie, C. J.; Sotofte, I.; Tuchagues, J.-P. *J. Chem. Soc., Dalton Trans.* **2005**, 1687−1692.
(59) Zheng, H.; Zang, Y.; Dong, Y.; Young, V. G.; Que, L. J. *J. Am. Chem. Soc.* **1999**, *121*, 2226−2235.
(60) Nanda, K. K.; Dutta, S. K.; Baitalik, S.; Venkatsubramanian, K.; Nag, K. *J. Chem. Soc., Dalton Trans.* **1995**, 1239−1244.
(61) Turowski, P. N.; Armstrong, W. H.; Liu, S.; Brown, S. N.; Lippard, S. J. *Inorg. Chem.* **1994**, *33*, 636−645.
(62) Ou, C.-C.; Lalancette, R. A.; Potenza, J. A.; Schugar, H. J. *J. Am. Chem. Soc.* **1978**, *100*, 2053−2057.
(63) Thich, J. A.; Ou, C. C.; Powers, D.; Vasiliou, B.; Mastropaolo, D.; Potenza, J. A.; Schugar, H. J. *J. Am. Chem. Soc.* **1976**, *98*, 1425−1433.
(64) Lee, D.; Pierce, B.; Krebs, C.; Hendrich, M. P.; Huynh, B. H.; Lippard, S. J. *J. Am. Chem. Soc.* **2002**, *124*, 3993−4007.
(65) Rohde, J.-U.; In, J. H.; Lim, M. H.; Brennessel, W. W.; Bukowski, M. R.; Stubna, A.; Munck, E.; Nam, W.; Que, L., Jr. *Science* **2003**, *299*, 1037−1039.
(66) Groves, J. T.; Haushalter, R. C.; Nakamura, M.; Nemo, T. E.; Evans, B. J. *J. Am. Chem. Soc.* **1981**, *103*, 2884−2886.
(67) Ye, W.; Ho, D. M.; Friedle, S.; Palluccio, T. D.; Rybak-Akimova, E. V. *Inorg. Chem.* **2012**, *51*, 5006−5021.
(68) Nam, W.; Jin, S. W.; Lim, M. H.; Ryu, J. Y. *Inorg. Chem.* **2002**, *41*, 3647−3652.
(69) Sastri, C. V.; Park, M. J.; Ohta, T.; Jackson, T. A.; Stubna, A.; Seo, M. S.; Lee, J.; Kim, J.; Kitagawa, T.; Munck, E.; Que, L., Jr.; Nam, W. *J. Am. Chem. Soc.* **2005**, *127*, 12494−12495.
(70) Nam, W. *Acc. Chem. Res.* **2007**, *40*, 522−531.
(71) Rhode, J.-U.; Que, L., Jr. *Angew. Chem., Int. Ed.* **2005**, *44*, 2255−2258.

(72) Hirao, H.; Kumar, D.; Que, L., Jr.; Shaik, S. *J. Am. Chem. Soc.* **2006**, *128*, 8590−8606.
(73) Schlichting, I.; Berendzen, J.; Chu, K.; Stock, A. M.; Maves, S. A.; Benson, D. E.; Sweet, R. M.; Ringe, D.; Petsko, G. A.; Sligar, S. G. *Science* **2000**, *287*, 1615−1622.
(74) Shirin, Z.; Young, V. G., Jr.; Borovik, A. S. *Chem. Commun.* **1997**, 1967−1968.
(75) Klinker, E. J.; Shaik, S.; Hirao, H.; Que, L., Jr. *Angew. Chem., Int. Ed.* **2009**, *48*, 1291−1295.
(76) Goldsmith, C. R.; Stack, T. D. P. *Inorg. Chem.* **2006**, *45*, 6048−6055.
(77) Pestovsky, O.; Bakac, A. *J. Am. Chem. Soc.* **2004**, *126*, 13757−13764.
(78) Warren, J. J.; Tronic, T. A.; Mayer, J. M. *Chem. Rev.* **2010**, *110*, 6961−7001.
(79) Neidig, M. L.; Wecksler, A. T.; Schenk, G.; Holman, T. R.; Solomon, E. I. *J. Am. Chem. Soc.* **2007**, *129*, 7531−7537.
(80) Lehnert, N.; Solomon, E. I. *J. Biol. Inorg. Chem.* **2003**, *8*, 294−305.